Electrochemical behaviour of some activated manganese ores

Julio B. Fernandes* and **Buqui D. Desai**
Department of Chemistry, Goa University, Bambolim, Goa 403 002 (India)

(Received June 25, 1990; in revised form September 11, 1990)

Abstract

Goan manganese ores, containing substantial amounts of Fe_2O_3 and SiO_2 have been subjected to activation treatment using H_2SO_4 and HNO_3 in varying concentration. The resulting oxides were characterised by chemical analyses, X-ray diffraction, and measurement of surface area. The discharge characteristics were evaluated in 9 M KOH solution. An attempt was made to correlate the structural features with the electrochemical activity. An explanation of the synergistic effect is given in the light of Ruetschi's cation vacancy model for manganese dioxides.

Introduction

Details of Goan natural manganese ore deposits and their utilisation have been extensively investigated [1–4]. The ore is essentially pyrolusite and psilomelane together with lesser amounts of cryptomelane, braunite and manganite. Details of the classification of natural manganese dioxide minerals with regard to crystal structure have been given by Burns and Burns [5]. We have reviewed [6] the various physicochemical principles involved in the activation of natural manganese ores on a previous occasion. The present investigation is aimed at evaluating the chemical and electrochemical characteristics of activated manganese dioxides in order to assess their suitability as active cathode materials in dry cells.

Experimental

The Goan manganese ores taken for activation treatment had the following initial composition :
G_1: Mn 50.4%, MnO_2 79.1%, Fe_2O_3 10.4%, SiO_2 9.3%;
G_2: Mn 57.1%, MnO_2 89.8%, Fe_2O_3 5.2%, SiO_2 4.8%.
Details of the activation process are given in Table 1. Chemical analysis of the activated samples was carried out using standard methods, reported

*Author to whom correspondence should be addressed.

0378-7753/91/$3.50

TABLE 1

Synthesis of activated ore samples

Sample	Quantities of reagents used in preparation[a]
D_1	Ore $G_1 \xrightarrow{\text{heat}} Mn_2O_3 \xrightarrow[10\%\ H_2SO_4]{300\ ml\ of} MnO_2$
D_2	Ore $G_1 \xrightarrow{\text{heat}} Mn_2O_3 \xrightarrow[10\%\ HNO_3]{300\ ml\ of} MnO_2$
D_3	Ore $G_1 \xrightarrow{\text{heat}} Mn_2O_3 \xrightarrow[30\%\ HNO_3]{300\ ml\ of} MnO_2$
D_4	Ore $G_2 \xrightarrow{\text{heat}} Mn_2O_3 \xrightarrow[30\%\ HNO_3]{300\ ml\ of} MnO_2$
D_5	Ore $G_2 \xrightarrow{\text{heat}} Mn_2O_3 \xrightarrow[35\%\ HNO_3]{300\ ml\ of} MnO_2$
D_6	Natural MnO_2 ore from Ghana (West Africa)

[a]In each case (D_1–D_5) 100 g of the ore was heated with 6% carbon black at 600 °C for 1 h.

elsewhere [7, 8]. X-ray powder diffractograms were taken on a Phillips X-ray machine using Cu Kα radiation. The discharge characteristics were evaluated in 9 M KOH solution at 1 mA constant current discharge per 100 mg of MnO_2 by a method reported earlier [9]. The usable energy values of the sample were evaluated by integrating the area under the closed circuit potential discharge curves at 1.0 V cut off [9]. The International Common Samples IC_1 (EMD) and IC_8 (CMD), and the chemically precipitated samples A_5 and A_6 [9], were used as standards for comparison of the data. Surface areas of the activated manganese ore samples were determined by the zinc ion absorption (ZIA) method at 65 °C [10]. The surface area of the active 'OH' groups was evaluated by the method of Brenet *et al.* [11, 12]. In this method each dioxide can be represented by the formula:

$$(MnO_2)_{2n-3}\,(MnOOH)_{4-2n}\cdot mH_2O$$

where

$$n=(3+x)/2 \quad \text{and} \quad x=0.632\times\ \%MnO_2/\%Mn$$

If M is the molecular mass for the above formula then the surface area of the OH group is given by

$$S_{OH}\equiv\ (4-2n)/M\times 3600\ m^2\ g^{-1}$$

The combined water percentage was determined by heating the samples (dried at 110 °C) to 300 °C and determining the loss in weight.

Results and discussion

The chemical composition and the formulae of the activated manganese dioxides are presented in Table 2. The X-ray diffraction data are presented

TABLE 2

Chemical composition and formulae of manganese dioxides

Sample	Yield (%)	MnO_2 (%)	Mn (%)	Fe (%)	x in MnO_{1+x}	Combined water (y) (%)	Formulae $(MnO_2)_{2n-3}(MnOOH)_{4-2n}mH_2O$
D_1	44.3	61.31	42.44	2.33	0.913	6.7	$(MnO_2)_{0.913}(MnOOH)_{0.087}0.3008\ H_2O$
D_2	54.2	61.45	42.63	1.56	0.911	5.7	$(MnO_2)_{0.911}(MnOOH)_{0.089}0.2453\ H_2O$
D_3	47.1	65.02	44.62	1.55	0.921	5.9	$(MnO_2)_{0.921}(MnOOH)_{0.079}0.2614\ H_2O$
D_4	44.5	76.85	51.50	3.50	0.943	10.7	$(MnO_2)_{0.943}(MnOOH)_{0.057}0.5476\ H_2O$
D_5	46.0	77.70	52.20	3.00	0.940	8.7	$(MnO_2)_{0.9407}(MnOOH)_{0.0593}0.4284\ H_2O$
D_6	–	80.30	52.47	1.37	0.970	2.8	$(MnO_2)_{0.9672}(MnOOH)_{0.0318}0.1451\ H_2O$
A_5	100.0	93.6	60.4	–	0.979	4.5	$(MnO_2)_{0.98}(MnOOH)_{0.021}0.21\ H_2O$
A_6	98.9	85.8	57.7	–	0.939	2.5	$(MnO_2)_{0.94}(MnOOH)_{0.07}0.093\ H_2O$
IC_1	–	90.0	60.3	–	0.95	2.85	$(MnO_2)_{0.95}(MnOOH)_{0.05}0.12\ H_2O$
IC_8	–	90.1	61.4	–	0.93	2.30	$(MnO_2)_{0.93}(MnOOH)_{0.07}0.08\ H_2O$

in Table 3. Samples D_1 and D_2, prepared by using 10% H_2SO_4 and 10% HNO_3, respectively, gave a low MnO_2 content (about 61%). When the concentration of HNO_3 was increased to 30%, as in the case of D_3, the MnO_2 content increased to about 65%. Samples D_4 and D_5 were obtained from a high grade ore (initial MnO_2 content = 89.8%) by disproportionation of the reduced ore in 30 and 35% HNO_3, respectively. The activated ores then showed a much higher percentage of MnO_2. It is interesting to note that all the activated ore samples have appreciably higher combined water contents than the standard electrolytic and chemical manganese dioxides (Table 2).

The X-ray diffraction data of all the activated samples conform to the γ crystal phase. The d values could generally be indexed on the basis of an orthorhombic crystal structure. The lattice parameters thus derived are in agreement with those reported in the literature [8, 13–15].

Sample discharge curves are displayed in Figs. 1 and 2 and their characteristics are summarised in Table 4. Sample D_4, obtained by disproportionation of the reduced ore in 30% HNO_3, showed a better discharge performance than D_5, which was similarly obtained using 35% HNO_3. This is in spite of the fact that D_5 had a higher percentage of MnO_2. This indicates that increasing the concentration of acid beyond 30% is not advisable as it results in samples having reduced activity. It is interesting to note at this stage that all the activated samples, including D_1 and D_2 (which have a very low MnO_2 content, 61%), show better discharge performance than D_6, a natural γ-MnO_2 ore (% MnO_2 = 80.3).

Discharge tests were also conducted by mixing activated ore samples with synthetic samples. Thus, when a mixture of A_5 (a chemical γ-MnO_2 with usable energy $E_u = 28.2$ J g^{-1}) and D_3 ($E_u = 12.2$ J g^{-1}) were used in a 1:1 combination, the resulting discharge performance was 25.2 J g^{-1} as

TABLE 3

X-ray diffraction data and lattice parameters of the activated ore samples

A_5		D_1		D_2		D_3		D_4		D_5		*hkl*
d (Å)	I/I_0	*d* (Å)	I/I_0	*d* (Å)	I/I_0	*d* (Å)	I/I_0	*d* (Å)	I/I_0	*d* (Å)	I/I_0	
4.1	42	4.04	12	3.90	30	3.9	30	4.00	48	3.96	5	110
		3.34	35	3.34	55	3.10	65					
		2.72	33	2.72	35	2.72	25					
		2.56	28									
2.41	45	2.42	36	2.45	44	2.42	86	2.42	70	2.42	75	021
		2.35	28	2.34	75	2.30	v.s					
2.11	58	2.13	7	2.12	35	2.13	88	2.12	45			
2.03	–	2.03	40	2.03	90	2.03	v.s			2.03	30	
1.63	100	1.645	100	1.625	100	1.635	100	1.625	100	1.635	100	221
				1.575	25							
1.425	21	1.43	27	1.436	40	1.43	–			1.43	90	022
Orthorhombic		Orthorhombic		Orthorhombic		Orthorhombic		Orthorhombic		Orthorhombic		
$a=4.435$ Å		$a=4.486$ Å		$a=4.383$ Å		$a=4.436$ Å		$a=4.387$ Å		$a=4.381$ Å		
$b=9.035$		$b=9.081$		$b=9.026$		$b=9.082$		$b=9.735$		$b=9.256$		
$c=2.85$		$c=2.86$		$c=2.87$		$c=2.86$		$c=2.789$		$c=2.852$		

Data of γ-MnO_2 sample A_5 [7, 8] is included for ready reference.

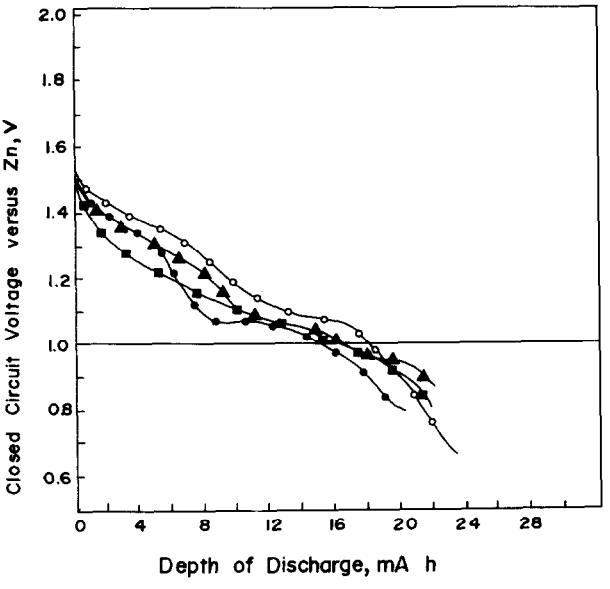

Fig. 1. Electrochemical discharge curves of activated ore sample in 9 M KOH solution. D_6 is a natural γ-MnO_2. D_1, —●—; D_3 —◀—; D_4 —○—; D_6 —■—.

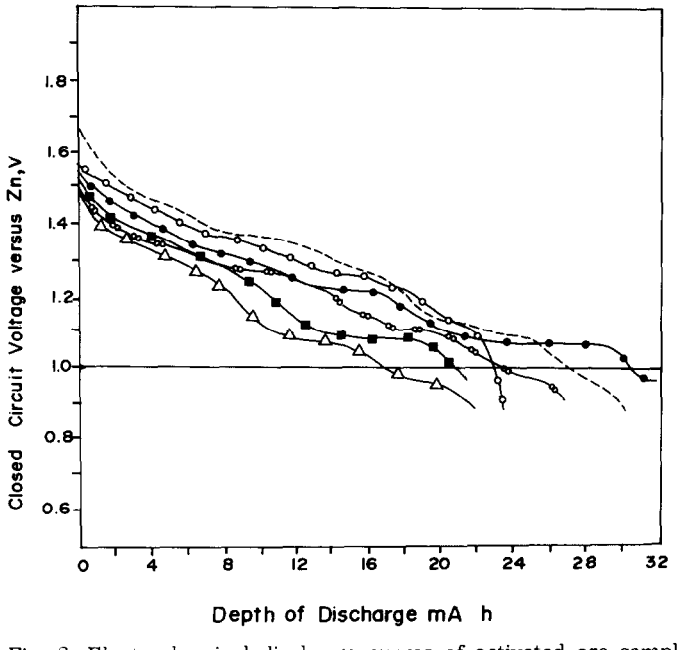

Fig. 2. Electrochemical discharge curves of activated ore samples in 9 M KOH solution. A comparative study with synthetic samples A_5 and the International Common Samples IC_1 and IC_8. D_3, —△—; A_5, -----; IC_1, —○—; IC_8, —○○—; D_3+A_5 (1:1), —●—; D_3+A_5 (3:1), —■—.

TABLE 4

Discharge characteristics of the manganese dioxides in 9 M KOH solution

Sample	Crystal phase	Open circuit voltage, OCV (V)		Closed circuit voltage, CCV (5 mA h) (V)	Polarisation, η (mV)			Discharge time at 1.0 V cut off (h)	Usable energy at 1.0 V cut off (J g^{-1})
		OCV (initial)	OCV (5 mA h)		η (5 mA h)	η (13 mA h)	η (21 mA h)		
D_1	γ	1.48	1.32	1.29	30	50	–	15.00	10.0
D_2	γ	1.48	1.325	1.300	25	55	–	14.00	10.1
D_3	γ	1.50	1.335	1.31	25	50	–	16.50	12.2
D_4	γ	1.52	1.375	1.35	25	20	–	18.3	15.0
D_5	γ	1.52	1.36	1.33	30	30	–	17.5	14.1
D_6	γ	1.50	1.365	1.215	150	265	–	16.3	9.63
A_5+D_3 (1:1)	γ	1.57	1.41	1.38	30	165	40	30.5	25.2
A_5+D_3 (1:3)	γ	1.52	1.37	1.35	20	20	–	21.0	16.0
A_5	γ	1.665	1.475	1.44	35	15	20	27.0	28.8
IC_1	γ	1.56	1.46	1.42	40	45	40	22.5	25.2
IC_8	γ	1.46	1.385	1.335	45	45	45	23.2	19.08

against the theoretically expected value of 20.5 J g^{-1}. The above combination therefore exhibits a synergistic effect [16]. In fact, the overall discharge performance was comparable with IC_1, one of the best electrolytic samples. Further, when only 25% of A_5 was used in combination with D_3, the resulting discharge capacity of 16.2 J g^{-1} was still good enough for use in the battery industry, especially considering the fact that IC_8, one of the best commercial γ-CMDs, has a capacity of only about 19 J g^{-1}, under the same conditions.

Recently, Ruetschi proposed a cation vacancy model [17] to explain the physical and electrochemical properties of γ- and ϵ-manganese dioxides. Accordingly, the general formulae of active manganese dioxides, i.e., $(MnO_2)_{2n-3}$ $(MnOOH)_{4-2n} \cdot mH_2O$ (see Table 2) can be represented by:

$$Mn_{(1-x-y)}^{4+} \cdot Mn_y^{3+} \cdot O_{(2-4x-y)}^{2-} \cdot OH_{(4x+y)}^{1-}$$

where x is the fraction of Mn^{4+} missing from the MnO_2 lattice resulting in Mn vacancies; y is the fraction of Mn^{4+} replaced by Mn^{3+}.

Since the cathodic reduction mechanism:

$$MnO_2 + H^+ + e^- \longrightarrow MnOOH$$

involves insertion of protons into the MnO_2 lattice, the electrochemical activity should obviously depend upon the rate of proton transfer from the Mn vacancy. It has been established [17] that the rate of proton transfer increases with the cation vacancy fraction, x, and attains a limiting value at $x = 0.25$. It is therefore very interesting to note that the value of x for the activated ore samples, which is between 0.10 and 0.22, is within the desired range (see Table 5). The value of x for chemical and electrolytic manganese dioxide is appreciably lower. Further, as shown in Fig. 3, a plot of usable energy versus x is linear, implying that the usable energy is directly proportional to the cation vacancy fraction, x. Higher x values beyond 0.25 could be detrimental, since it would result in much higher structural water [17] and, hence, lower electrochemical activity.

TABLE 5

Correlation of structural features with the catalytic and electrochemical activity of the samples

	Surface areas (m^2 g^{-1})		Usable energy (J g^{-1})	Cation vacancy fraction (X)
	ZIA	S_{OH}		
D_1	105	33.8	10.0	0.130
D_2	110	35.0	10.1	0.109
D_3	121	31.0	12.2	0.116
D_4	132	21.0	15.0	0.215
D_5	126	22.5	14.1	0.1764
D_6	12.8	12.7	9.63	0.067
A_5	44	8.3	28.8	0.095
A_6	46	29.0	12.5	–
IC_1	88	20.0	25.2	–
IC_8	98	28.0	19.0	0.038

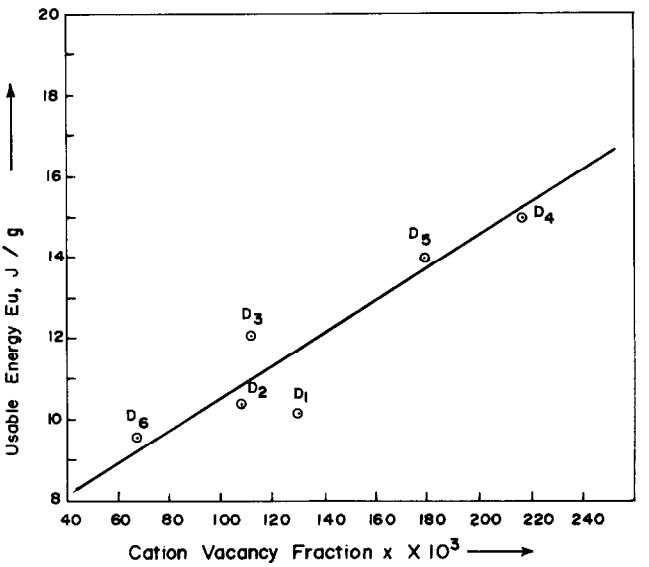

Fig. 3. Relation between usable energy and cation vacancy fraction in manganese dioxides.

It should be obvious, however, that the value of x cannot be treated as a measure of electrochemical activity, but only as an influencing factor to favour proton transfer during electrochemical reduction. If this assumption is correct, then the synergistic effect of the $(A_5 + D_3)$ combination could be due to the favourable effect of the higher x value of D_3 ($x = 0.116$) on the discharge performance of the more electrochemically active A_5($x = 0.095$). Also, the apparent lack of correlation (see Table 5) or, rather, the somewhat inverse relation between the surface area of the 'OH' groups and the electrochemical activity, could be due to the failure of Brenet *et al.* [11, 12] to account for the two types of OH groups, corresponding to planar and pyramidal configurations of O^{2-} sites, as envisaged in Ruetschi's cation vacancy model. This aspect is being investigated further by the present authors and details will be communicated at a later stage.

Conclusions

The activated ore samples have unusually high surface areas compared with chemical or electrolytic manganese dioxides. Further, the samples, even with very low MnO_2 contents, can show a synergistic effect, thus emphasizing their immense importance to the battery industry. A reason for the synergistic effect can be given on the basis of Ruetschi's cation vacancy model for manganese dioxides.

References

1 A. R. Gokul, *Indian Miner.*, *29* (1974) 1.
2 A. G. Desai and V. V. Peshwa, *Proc. Symp. Morph. Evol. Landforms, New Delhi, 1978*, Geological Survey of India, New Delhi, 1978, p. 255.
3 A. G. Desai and G. G. Deshpande, *Geoviews*, *5* (1979) 21.
4 B. D. Desai, *Ph. D. Thesis*, Univ. Bombay, India, 1980.
5 V. M. Burns and R. G. Burns, in A. Kozawa and R. J. Brodd (eds.), *Proc. MnO_2 Symp., Cleveland, OH, U.S.A., 1975*, Vol. 1, I.C. Sample, Parma Technical Centre, Cleveland, OH, U.S.A., p. 288.
6 J. B. Fernandes, B. D. Desai and V. N. Kamat Dalal, *J. Power Sources*, *15* (1985) 209.
7 J. B. Fernandes, *Ph. D. Thesis*, Univ. Bombay, India 1983.
8 J. B. Fernandes, B. D. Desai and V. N. Kamat Dalal, *Electrochim. Acta*, *28* (1983) 309.
9 J. B. Fernandes, B. D. Desai and V. N. Kamat Dalal, *Electrochim. Acta*, *29* (1984) 181.
10 A. Kozawa, in K. V. Kordesch (ed.), *Batteries, Manganese Dioxide*, Vol. 1, Marcel Dekker, New York, 1974, p. 497.
11 J. B. Brenet, K. Traore, M. Cyrankowska, G. Ritzer and R. Saka, in A. Kozawa and R. J. Brodd (eds.), *Proc. MnO_2 Symp., Cleveland, OH, U.S.A., 1975*, Vol. 1, I.C. Sample, Parma Technical Centre, Cleveland, OH, U.S.A., p. 264.
12 J. B. Brenet, K. Traore and Kappler, in A. Kozawa and R. J. Brodd (eds.), *Proc. MnO_2 Symp., Cleveland, OH, U.S.A., 1975*, Vol. 1, I.C. Sample, Parma Technical Centre, Cleveland, OH, U.S.A., p. 290.
13 R. Giovanoli, R. Maurer and W. Feitneckt, *Helv. Chim. Acta*, *50* (1967) 1972.
14 P. M. de Wolff, *Acta Crystallogr.*, *12* (1959) 341.
15 M. Bystrom, *Acta Chem. Scand.*, *3* (1949) 163.
16 J. Y. Welsh and P. Picquet, *Prog. Batteries Solar Cells*, *2* (1979) 119.
17 P. Ruetschi, *J. Electrochem. Soc.*, *131* (1984) 2737.